

# Theoretical Bases of A Thermo-Mechanical Damage and DMT-Healing Model for Rock

C. Zhu<sup>1</sup> and C. Arson<sup>2</sup>

<sup>1</sup>Ph.D. student, School of Civil and Environmental Engineering, Georgia Institute of Technology, Mason Building, 790 Atlantic Drive, Atlanta, GA 30332-0355. Email: chengzhu@gatech.edu

<sup>2</sup>ASCE member, Ph.D., Assistant Professor, School of Civil and Environmental Engineering, Georgia Institute of Technology, Mason Building, 790 Atlantic Drive, Atlanta, GA 30332-0355. Email: chloe.arson@ce.gatech.edu

**ABSTRACT:** A theoretical framework is proposed to model thermo-mechanical (TM) crack opening, closure, and healing in rock. The model is based on Continuum Damage Mechanics and thermodynamics. The postulated free energy is a polynomial of deformation, temperature, damage and healing. The damage-driving force captures damage evolution due to mechanical or TM tensile stresses, as well as the decrease of material toughness at elevated temperature. Crack closure is modeled by adopting the concept of unilateral effect on rock stiffness. A mixed variable is introduced to account for anisotropic TM damage and rate-dependent healing. Crack rebonding is assumed to result from Diffusive Mass Transfer (DMT) processes, and accordingly, the healing evolution law is governed by the diffusion equation. Contrary to other models for rock, the healing deformation is not a creep volumetric deformation, but the difference between the deformation before and after DMT. A parametric study illustrates the model capabilities: the simulation of TM stress paths with higher degree of mechanical recovery for longer healing time or higher healing temperature. The proposed model is expected to better predict the long-term behavior of self-healing rock materials – containing clay of halite minerals for instance.

## 1. INTRODUCTION

Cavities, hydraulic fractures and faults resulting from excavation, high-pressure fluid injection and forced tectonic processes are surrounded by damaged zones. In addition to mechanical stresses, rock around underground nuclear waste repositories and geothermal systems is also subjected to important temperature gradients, which can significantly affect its mechanical and physical properties (Zhu and Arson, 2013). Moreover, geological formations containing clay or halite minerals exhibit a self-healing behavior under constant stress and temperature conditions. As a result, redistribution of stress and temperature changes within the rock mass can induce localizations leading to crack opening, closure, and rebonding. However, stress reorientation often gives cracks a preferential orientation. Resulting damage-induced anisotropy of stiffness raises major thermodynamic issues in a Continuum Damage Mechanics (CDM) framework (Chaboche, 1992). Healing induced by crack rebonding brings the additional challenge of the definition of thermodynamic dissipation variables (Arson et al., 2012). Most damage and healing models proposed in rock thermo-mechanics are based on the concept of dilatancy boundary (Hou, 2003). Anisotropic healing models based on CDM usually resort to the concept of “net damage” (Barbero et al., 2005), which allows modeling stiffness decrease

(damage) and increase (healing). Existing rock damage models distinguishing two modes of healing (closure and rebonding) conveniently resort to rate-dependent evolution laws for all dissipation variables, which avoids the challenges associated to the requirement on the positivity of dissipation (Chan et al., 1998). However, such models do not properly represent the evolution of brittle behavior associated to rate-independent crack opening and closure, and actually consider healing as a particular form of crack closure (detected by an increase of wave velocity) rather than crack rebonding. The goal of this research work is to enrich a continuum thermo-mechanical (TM) model of anisotropic damage with a healing variable representing DMT-induced crack rebonding, in order to predict rock stiffness and deformation during TM crack opening, closure and rebonding. The theoretical framework is explained in Section 2. Section 3 presents stress/strain curves and the evolution of damage and healing variables during anisotropic TM stress paths.

## 2. THEORETICAL FRAMEWORK

### 2.1 Thermo-mechanical (TM) stress induced crack opening and closure

The proposed constitutive model is formulated to couple crack opening, closure, and healing within the framework of CDM. The strain energy loss due to crack propagation is used to compute damaged stiffness and deformation. The second order crack density tensor defined by Kachanov (1992) is adopted in the energy dissipation expression. For irreversible material behavior, state equations must be completed with the laws governing the evolution of internal variables and the associated dissipative mechanisms. In most CDM models for rocks, the damage potential is assumed to be equal to the damage criterion. Moreover, the free energy expression is chosen so as to allow residual strains after stress relaxation without introducing any additional plastic potential. This economical thermodynamic model relies on two postulates only. In the present work, the anisotropic CDM model of crack opening formulated by Dragon et al. (2000) is used as a basis for the TM damage model (Table 1).

Assuming that undamaged rock has a linear thermo-elastic behavior, the free energy of the damaged rock solid skeleton is expressed as a polynomial of order 2 in elastic deformation  $\boldsymbol{\varepsilon}^E$  and order 1 in temperature change  $\tau$ . The damage criterion is expressed as the difference between the norm of the energy release rate and an energy threshold. The total deformation tensor is split into three components: purely elastic deformation ( $\boldsymbol{\varepsilon}^e$ ), damage induced elastic deformation ( $\boldsymbol{\varepsilon}^{ed}$ ), and damage induced irreversible deformation ( $\boldsymbol{\varepsilon}^{id}$ ). Conjugation relationships derived from thermodynamic principles give stress and the energy release rate. The latter can be further decomposed into two parts:  $\mathbf{Y}_1$  accounts for crack propagation;  $\mathbf{Y}_2$  describes rock property changes due to temperature variation. Only certain components of the thermodynamic variable conjugate to damage ( $\mathbf{Y}$ ) have an influence on the damage growth: the TM tensile damage-driving force ( $\mathbf{Y}_{1a}^+ = -g\boldsymbol{\varepsilon}^+$ ) and the thermal damage-driving force ( $\mathbf{Y}_2^d$ ). A dimensional analysis indicates that the term  $\frac{1}{2\tau_0} \frac{\partial C(\Omega)}{\partial \Omega} \tau^2$  is negligible compared to  $\tau \frac{\partial K(\Omega)}{\partial \Omega} : \boldsymbol{\varepsilon}^E$ .  $\mathbf{Y}_2^d = A \cdot \tau \cdot \alpha_T (\alpha + 2\beta) \text{tr}(\boldsymbol{\varepsilon}^{E+})$ , is defined to account for the decrease of rock toughness as temperature increases.

**TABLE 1. Outline of thermo-mechanical damage and healing model**

<b>Postulates</b>			
Free Energy for Crack Opening ( $\Psi_S$ )	$\Psi_S(\boldsymbol{\varepsilon}^E, \tau, \boldsymbol{\Omega}) = \frac{1}{2} \boldsymbol{\varepsilon}^E : \mathbf{D}(\boldsymbol{\Omega}) : \boldsymbol{\varepsilon}^E + g\boldsymbol{\Omega} : \boldsymbol{\varepsilon} - \frac{1}{2\tau_0} C(\boldsymbol{\Omega})\tau^2 - \tau \mathbf{K}(\boldsymbol{\Omega}) : \boldsymbol{\varepsilon}^E$ $\frac{1}{2} \boldsymbol{\varepsilon}^E : \mathbf{D}(\boldsymbol{\Omega}) : \boldsymbol{\varepsilon}^E = \frac{1}{2} \lambda (\text{tr} \boldsymbol{\varepsilon}^E)^2 + \mu \text{tr}(\boldsymbol{\varepsilon}^E \cdot \boldsymbol{\varepsilon}^E) + \alpha \text{tr} \boldsymbol{\varepsilon}^E \text{tr}(\boldsymbol{\varepsilon}^E \cdot \boldsymbol{\Omega}) + 2\beta \text{tr}(\boldsymbol{\varepsilon}^E \cdot \boldsymbol{\varepsilon}^E \cdot \boldsymbol{\Omega})$		
Free Energy for Crack Closure ( $\Psi_S$ )	$\Psi_S(\boldsymbol{\varepsilon}^E, \tau, \boldsymbol{\Omega}) = \frac{1}{2} \boldsymbol{\varepsilon}^E : \mathbf{D}_{eff}(\boldsymbol{\Omega}) : \boldsymbol{\varepsilon}^E + g\boldsymbol{\Omega} : \boldsymbol{\varepsilon} - \frac{1}{2\tau_0} C_{eff}(\boldsymbol{\Omega})\tau^2 - \tau \mathbf{K}_{eff}(\boldsymbol{\Omega}) : \boldsymbol{\varepsilon}^E$ $\mathbf{D}_{eff}(\boldsymbol{\Omega}) = \mathbf{D}(\boldsymbol{\Omega}) + \eta \sum_{i=1}^3 H(-\text{tr}(\mathbf{P}_i : \boldsymbol{\varepsilon})) \mathbf{P}_i : (\mathbf{D}_0 - \mathbf{D}(\boldsymbol{\Omega})) : \mathbf{P}_i, 0 < \eta \leq 1$ $\mathbf{K}_{eff}(\boldsymbol{\Omega}) = \mathbf{K}(\boldsymbol{\Omega}) + \eta \sum_{i=1}^3 H(-\text{tr}(\mathbf{P}_i : \boldsymbol{\varepsilon})) \mathbf{P}_i : (\mathbf{K}_0 - \mathbf{K}(\boldsymbol{\Omega})) : \mathbf{P}_i, 0 < \eta \leq 1$ $C_{eff}(\boldsymbol{\Omega}) = C(\boldsymbol{\Omega}) + \eta \sum_{i=1}^3 H(-\text{tr}(\mathbf{P}_i : \boldsymbol{\varepsilon})) \mathbf{P}_i : [(C_0 - C(\boldsymbol{\Omega})) \boldsymbol{\delta} \otimes \boldsymbol{\delta}] : \mathbf{P}_i, 0 < \eta \leq 1$		
Free Energy for Crack Rebonding ( $\Psi_S$ )	Replace $\boldsymbol{\Omega}$ by $\mathbf{A}$ in the free energy for crack closure $\mathbf{A} = \boldsymbol{\Omega} - \boldsymbol{\delta} h$		
Damage Criterion for Crack Opening, Closure and Rebonding ( $f_d$ )	$f_d(\mathbf{Y}_d^+, \boldsymbol{\Omega}) = \sqrt{\frac{1}{2} \mathbf{Y}_d^+ : \mathbf{Y}_d^+} - [C_0 + C_1 \text{Tr}(\boldsymbol{\Omega})]$		
Strain Decomposition	$\boldsymbol{\varepsilon} = \boldsymbol{\varepsilon}^e + \boldsymbol{\varepsilon}^{ed} + \boldsymbol{\varepsilon}^{id} = \boldsymbol{\varepsilon}^E + \boldsymbol{\varepsilon}^{id} = \boldsymbol{\varepsilon}^{EM} + \boldsymbol{\varepsilon}^{ET} + \boldsymbol{\varepsilon}^{id}$		
Diffusion Equation	$\bar{u}(t) = \frac{8U_0}{\pi L_{REV}} \sum_{i=1,3,5,\dots}^{\infty} \frac{e^{-\lambda_n^2 D t}}{n \lambda_n}, \lambda_n = \frac{n\pi}{x_{max}}$ $h(t) = 1 - \bar{u}(t)$		
<b>Conjugation relationships</b>			
Stress ( $\boldsymbol{\sigma}$ )	$\boldsymbol{\sigma} = \frac{\partial \Psi_S(\boldsymbol{\varepsilon}^E, \tau, \boldsymbol{\Omega})}{\partial \boldsymbol{\varepsilon}^E} = \mathbf{D}(\boldsymbol{\Omega}) : \boldsymbol{\varepsilon}^E + g\boldsymbol{\Omega} - \tau \mathbf{K}(\boldsymbol{\Omega})$		
Damage Driving Force ( $\mathbf{Y}_d^+$ )	$\mathbf{Y} = -\frac{\partial \Psi_S(\boldsymbol{\varepsilon}^E, \tau, \boldsymbol{\Omega})}{\partial \boldsymbol{\Omega}} = \mathbf{Y}_1 + \mathbf{Y}_2$ $\mathbf{Y}_1 = -g\boldsymbol{\varepsilon} - \alpha(\text{tr} \boldsymbol{\varepsilon})\boldsymbol{\varepsilon} - 2\beta(\boldsymbol{\varepsilon} \cdot \boldsymbol{\varepsilon}), \mathbf{Y}_2 = \frac{1}{2\tau_0} \frac{\partial C(\boldsymbol{\Omega})}{\partial \boldsymbol{\Omega}} \tau^2 + \tau \frac{\partial \mathbf{K}(\boldsymbol{\Omega})}{\partial \boldsymbol{\Omega}} : \boldsymbol{\varepsilon}^E$ $\mathbf{Y}_d^+ = -g\boldsymbol{\varepsilon}^+ + \mathbf{A} \cdot \tau \cdot \alpha_T (\alpha + 2\beta) \text{tr}(\boldsymbol{\varepsilon}^{E+})$		
$\boldsymbol{\varepsilon}^{EM}$	= mechanical deformation component	$\boldsymbol{\varepsilon}^{ET}$	= thermal deformation component
$\alpha, \beta$	= mechanical damage parameters	$C_0$	= initial damage threshold
$\lambda, \mu$	= Lamé coefficients	$C_1$	= damage hardening parameter
$\tau_0$	= initial temperature	$g$	= toughness parameter
$\mathbf{D}$	= damaged stiffness tensor	$k$	= bulk modulus
$\alpha_T$	= thermal expansion coefficient	$\mathbf{K}$	= $k\alpha_T$ "diagonal tensor"
$\mathbf{D}_{eff}$	= effective stiffness tensor after "partial recovery"	$C$	= damaged heat capacity
$\mathbf{K}_{eff}$	= effective diagonal tensor after "partial recovery"	$\mathbf{A}$	= TM damage parameter
$C_{eff}$	= effective heat capacity after "partial recovery"	$\eta$	= degree of maximum stiffness recovery
$\mathbf{P}_i$	= 4 <sup>th</sup> order project tensor for the projection in crack planes normal to direction $i$	$\boldsymbol{\delta}$	= second order identity tensor

In CDM, unilateral effects refer to the recovery of material compressive strength due to the closure of tensile cracks. Following Chaboche's (1992) approach, the expression of stiffness depends on a Heaviside function ( $H$ ) to distinguish behaviors in tension and compression. The damage criterion needs to be changed so that compressed rock behaves like the pristine rock material under compression, as soon as the cracks perpendicular to the direction of compression are closed (Table 1). In this study, it is assumed that full compressive strength recovery is achieved ( $\eta = 1$ ) if all cracks are closed under compression. More details can be found in a previous study by Zhu and Arson (2013).

## 2.2 Creep-induced healing

Healing in rock is expected to occur due to Diffusive Mass Transfer (DMT) processes. In the absence of saturating fluids, cracks can only heal if faces are in contact. In this model, healing is therefore constrained to occur only if cracks are closed. Most of the papers dealing with DMT healing described healing as the time-dependent counter-effect of dilatant cracking, and therefore introduced a visco-plastic creep law to predict healing deformation (e.g., Senseny et al., 1992). The rate-dependent damage and healing variables introduced to explain the time-dependence of the elastic moduli during creep represent the same physical processes as the macroscopic deformation creep laws used to capture damage and healing deformation - such as in the dilatancy-boundary model proposed by Hou (2003). In CDM however, “healing” means “mechanical recovery associated to crack rebonding”. Therefore, it cannot be captured solely by a deformation component: another dissipation variable needs to be introduced (Arson et al., 2012). Previous CDM healing models resort to net damage to model “counter-effects” of damage, leading to mechanical stiffness recovery (e.g. Voyiadjis et al. 2012). CDM healing models can in theory be used for rate-independent and rate-dependent processes (Miao et al., 1995).

DMT processes leading to crack rebonding may be thought of the migration of ions from the intact rock lattice to crack faces. Electronic attraction forces between different ionic species at crack faces seal the cracks. At the scale of a typical rock sample ( $\sim 10^{-2}$  m), diffusion is essentially an isotropic phenomenon. Therefore, we propose to model mechanical stiffness recovery by a mixed damage variable  $\mathbf{A}$  (similar to net damage), defined as the difference between the CDM anisotropic damage tensor  $\mathbf{\Omega}$  and an isotropic healing variable  $h$ :

$$\mathbf{A} = \mathbf{\Omega} - \delta h \quad (1)$$

In which  $\delta$  is the second-order identity tensor. After the healing process, the damaged stiffness tensor should depend on  $\mathbf{A}$  instead of  $\mathbf{\Omega}$ . A general diffusion equation is assumed to govern the kinetics of healing:

$$\frac{\partial u}{\partial t} = D \nabla^2 u \quad (2)$$

In which  $u = U_0 - h$  is further referred to as the “density of net damage”.  $D$  is the diffusion coefficient.  $U_0$  is the initial density of damage in the Representative Elementary Volume (REV), before healing occurs:  $U_0 = Tr(\mathbf{\Omega})_{t=0}$ .

In the proposed model, damage is defined at the centimeter scale, for a REV representing a typical rock sample ( $L_{REV} \sim 10^{-2}$  m). The diffusion equation above depends on a microscopic space gradient, which represents the heterogeneity of rock structure within the REV. The proposed model is a particular gradient-enhanced model depending on an internal length parameter ( $x_{max}$ ) representing the average crack spacing within the REV (note that both open and closed cracks are included in the pattern to compute the average spacing). When an ion reaches a crack face, electronic forces bonds this ion to the lattice of the opposite crack face, and therefore, healing at this face is assumed to be complete. Therefore the diffusion equation above should be solved for the following boundary conditions:  $u(x = 0, t) = 0, u(x = x_{max}, t) = 0$ . For a given time, it is assumed that all cracks in the REV are subjected to the same rate of healing. Therefore, the initial condition that should be considered

to solve the diffusion equation is the same as the initial condition of damage at the REV scale:  $u(x, t = 0) = U_0$ . The space average of the density of net damage can be defined at the REV scale as:

$$\bar{u}(t) = \langle u(x, t) \rangle = \frac{1}{x_{max}} \int_0^{x_{max}} u(x, t) dx = \frac{8U_0}{\pi x_{max}} \sum_{i=1,3,5,\dots}^{\infty} \frac{e^{-\lambda_n^2 D t}}{n \lambda_n}, \quad \lambda_n = \frac{n\pi}{x_{max}} \quad (3)$$

For the normalized solution ( $U_0 = 1$ ), as time evolves,  $\bar{u}(t)$  approaches zero. Ultimately, healing is complete when the normalized time  $\tilde{t}$  reaches one, i.e. when time gets equal to the characteristic time  $t = \frac{(x_{max})^2}{D}$ . Note that the diffusion coefficient  $D$  only varies with temperature in this study, in order to put the emphasis on the influence of temperature on DMT processes. Taking the general expression of diffusion for solids as a starting point:

$$D = D_0 e^{-\frac{Q}{RT}} \quad (4)$$

In which  $D_0$  is the maximum diffusion coefficient (at infinite temperature),  $Q$  is the activation energy,  $T$  is temperature,  $R$  is the constant of perfect gases. Since DMT processes are particularly salient in salt rock, the study of ion diffusion through solid *NaCl* by Yu and Fuji (2000) is used to express  $D$  as a function of temperature:

$$D = 10^{8.8099} e^{-\frac{28710.93}{T}} \quad (5)$$

In which  $T$  is expressed in Kelvin. Note that the formula above was fitted to experimental results obtained during diffusion tests performed on salt within the range of temperature 723K – 813K. For the simulations presented in the following, a standard value of diffusion measured in salt rock at room temperature ( $D=10^{-16}$  m<sup>2</sup>/s) is adopted for cases simulated at room temperature (293K), while formula in Eq. 5 above is extrapolated for the range of elevated temperatures (553K and 573K).

### 2.3 Integration of TM effects of crack opening, closure and rebonding

Damage is a rate-independent dissipation variable. Consistency equations impose that damage cannot decrease. Crack closure can be seen as the elastic deformation associated to the normal displacement of open crack faces under compression. Healing associated to crack rebonding requires an energy input (to trigger the migration of ions within the lattice), and is therefore a dissipative process independent from damage (Arson et al., 2012). As a result, the free energy of the REV should now depend on two state variables (elastic deformation and temperature) and two dissipation variables (damage  $\Omega$  and healing  $h$ ). The general formulation of the model is also shown in Table 1.

The CDM healing variable  $h$  is related to healing-induced deformation, defined as a “counter-acting” damage deformation. To illustrate the concept, a hypothetical stress/strain curve is provided (Fig. 1) for the stress path shown in Fig. 2. The specimen is subjected to tension and behaves elastically (OA) until damage starts to develop (AB). When tensile stress is released (BC), no additional damage is produced, but residual crack opening induce irreversible damage deformation (distance OC). The latter can be compensated by applying further compression (CD). At state D, all tensile cracks are closed. As a result, compression beyond that point (DE) exhibits

unilateral effects. At E, the sample is maintained at constant stress for a certain amount of time, inducing DMT healing phase (EF). Then the sample is reloaded in tension. As long as the sample is in compression (FG), the slope of the stress/strain curve is equal to the original slope (OA). Once in tension again, the stress/strain curve (GH) exhibits a form similar to branch (OAB). The slope of the linear segment on GH should be steeper than the slope of segment BC due to healing process. For a given state of stress after a loading/unloading/creep/reloading cycle ( $\sigma_1$  in Fig. 1), the healing deformation ( $\varepsilon^h$ ) is defined as the difference between deformation in the absence of healing, and the deformation observed after DMT has occurred.

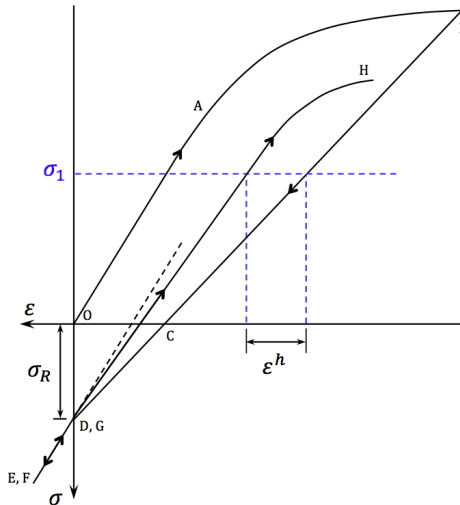


**FIG. 1** Hypothetical stress/strain curve for the stress path illustrated in Fig. 2.

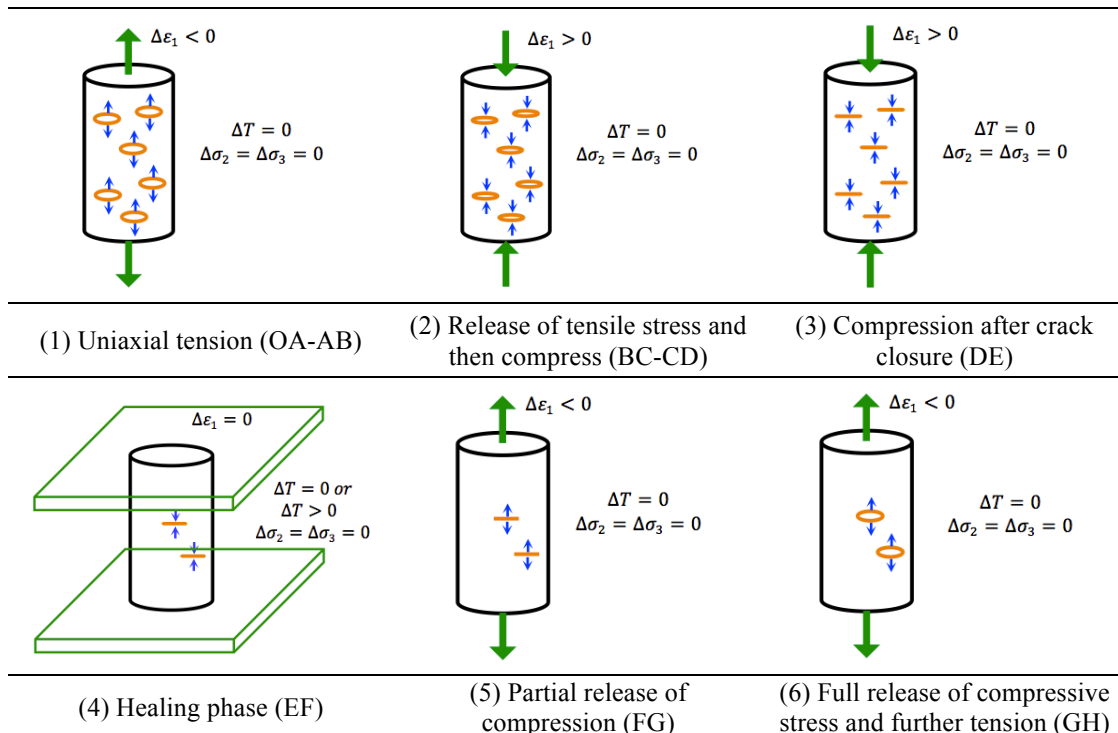


**FIG. 2** Stress path simulated for TM crack opening, closure and healing.

### 3. SIMULATION

The stress path illustrated in Fig. 2 is simulated at the integration point (with MATLAB) for a unit REV ( $L_{REV} = 1m$ ). The diffusion equation solution averaged in space (Eq. 3) is approximated by truncating the infinite sum at  $N=100$ . The proposed theoretical model depends on 7 mechanical parameters  $\lambda, \mu, \alpha, \beta, g, C_0, C_1$ , 1 thermal parameter  $\alpha_T$ , and 2 diffusion parameters  $U_0, x_{max}$ . To the authors' best knowledge, there is no experimental data available to date allowing the calibration of anisotropic damage parameters for salt rock. Mechanical and damage parameters are taken from the calibration work done by Dragon et al. (2000) for the Fontainebleau sandstone. Sandstone generally follows a brittle behavior. Salt rock usually deforms to a relatively large extent before failure. The stress/strain response of sandstone is therefore expected to exhibit larger strength and less deformation than salt rock. Since  $\mathbf{K}(\boldsymbol{\Omega})$  depends on the damaged stiffness tensor, the thermal expansion coefficient  $\alpha_T$  can be considered as a purely thermo-elastic parameter. Therefore, a standard value for rock materials is assigned to  $\alpha_T$  in this study. Table 2 summarizes the material parameters used. The soil mechanics sign convention is adopted here with tension in negative.

**Table 2. Material parameters used in the simulations**

$\lambda$ (Pa)	$\mu$ (Pa)	$\alpha$ (Pa)	$\beta$ (Pa)	$U_0$
$2.63 \times 10^{10}$	$1.75 \times 10^{10}$	$1.9 \times 10^9$	$-2.4 \times 10^{10}$	1
$g$ (Pa)	$C_0$ (Pa)	$C_1$ (Pa)	$\alpha_T$ ( $K^{-1}$ )	$x_{max}$ (m)
$1.1 \times 10^8$	1000	$5.5 \times 10^5$	$-1 \times 10^{-5}$	$1 \times 10^{-4}$

To emphasize on the impact of duration and temperature on the recovery of material strength, 5 scenarios are considered for the healing phase. Scenario 1 is taken as the reference healing case with a 200s duration at room temperature ( $T_{room} = 293K$ ). Scenarios 2 and 3 are carried out at room temperature but for longer healing periods (2000s, 20000s). In scenarios 4 and 5, healing occurs at an elevated temperature (553K, 573K) for the same period of time as in the reference case. For all scenarios, the mechanical loading and unloading phases are carried out at  $T_{room}$ .

#### 3.1 Influence of time on healing (Scenarios 1, 2, and 3)

During the rate-independent uniaxial tension phase, a maximum axial strain of  $\varepsilon_1 = -0.0009$  is applied incrementally (Fig. 3.a). Rock is weak in tension, so damage starts to develop quickly after the initiation of the tensile loading. Consequently, linear stress-strain response is observed for a very short interval only (OA), after which the curve becomes nonlinear (AB). To compensate the damaged deformation, the sample is unloaded and further compressed elastically without producing any new cracks (BC-CD). Tensile-induced cracks are fully closed at D. Due to the assumptions made in the model to account for unilateral effects, the slope of line DE (under additional compression) is the same as the slope of line OA (undamaged stiffness).

The healing phase is started for a compressive strain of  $\varepsilon_1 = 0.001$  (this value is chosen so as to prevent the initiation of lateral damage ( $\Omega_3$ ) under compression). The

healing period (E-F) affects rate-dependent mechanical recovery. The decrease of DMT-induced density of net damage ( $u$ ) follows the ordered sequence:  $u_1 > u_2 > u_3$  (where the subscript refers to the scenario simulated; Fig. 3.b). For all scenarios, the damage variable keeps increasing and only becomes constant during the unloading and healing phases (Fig. 3.c). Note that according to the theoretical model formulation, the net damage variable ( $\mathbf{A}$ ) decreases during healing (Fig. 3.d), but the damage variable ( $\mathbf{\Omega}$ ) does not. After healing, the sample is unloaded again to its original length (FG) and then subjected to axial tension again (GH). Larger healing induces higher mechanical recovery. Accordingly, the slope of the reloading curve is steeper for scenario 3 (resp. 2) than scenario 2 (resp. 1). The damage criterion depends on a strain threshold, which is not made dependent on healing (Table 1). So the sample is re-damaged for the same tensile strain during reloading (Fig. 3.a). The proposed model predicts that the yield stress is higher for a partially healed sample than for an undamaged sample: this part of the model formulation will be improved in further developments. This artifact is due to the account of irreversible damage-induced deformation in the model.

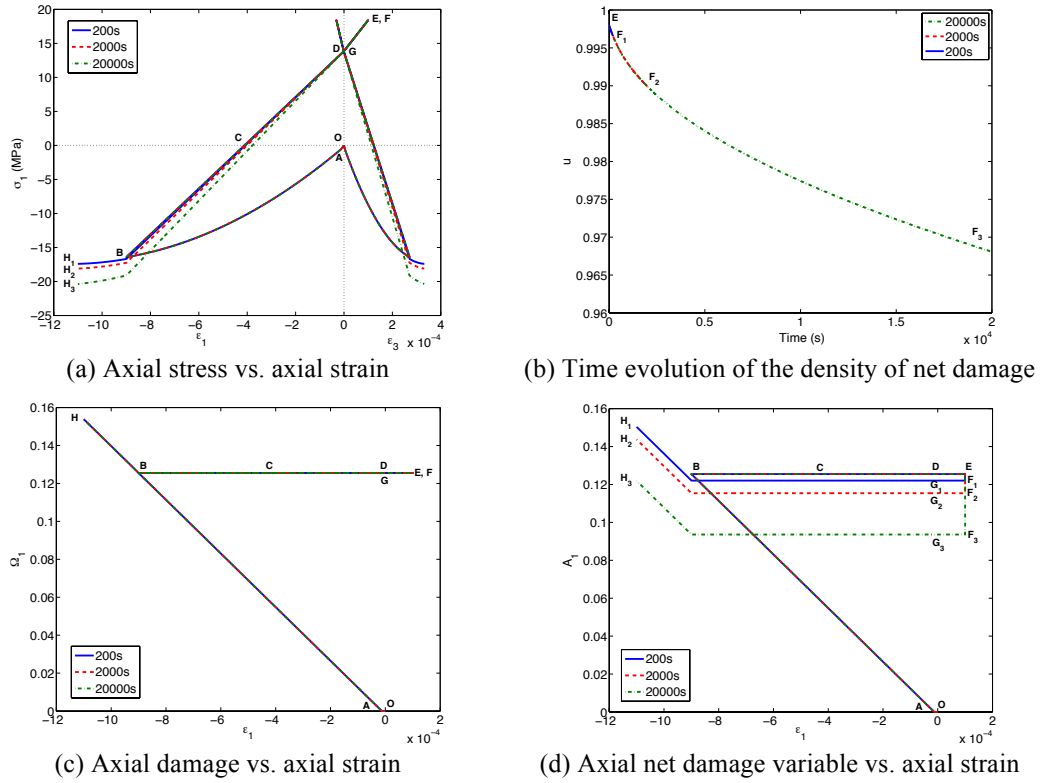


**FIG. 3 Stress path simulated at room temperature for three healing periods.**

### 3.2 Influence of ambient temperature on healing (Scenarios 4 and 5)

The same loading path is repeated for Scenarios 4 and 5, with higher temperature during healing (E-F): the temperature increase (resp. 260K, 280K) is applied in one step (resp. E<sub>1</sub>-E<sub>4</sub>, E<sub>1</sub>-E<sub>5</sub>), so that healing occurs at constant temperature. The healing period is same as in the reference case (200s). The subsequent reloading phases (FG

and GH) are simulated at room temperature (293K). The general shape of the stress-strain curve is similar to the previous scenarios. During the healing phase, the sample tends to expand (both laterally and axially) because of the temperature increase (thermal dilation). Displacements in the axial direction are fixed, which results in the development of compressive stress ( $E_1$ - $E_4$ ,  $E_1$ - $E_5$  in Fig. 4.a). According to the model formulation, DMT- induced decrease of net damage ( $u$ ) is more important at higher temperature (Fig. 4.b). Given the same healing period, temperature increments of 0K, 260K, and 280K decrease the damage variable by 2.7%, 34.4% and 85.1% respectively (Fig. 4.d). To achieve the same healing effect, it requires a significantly less healing time at high temperature. The evolution of damage variable remains unchanged since it is associated with the mechanical loading path (Fig. 4.c).

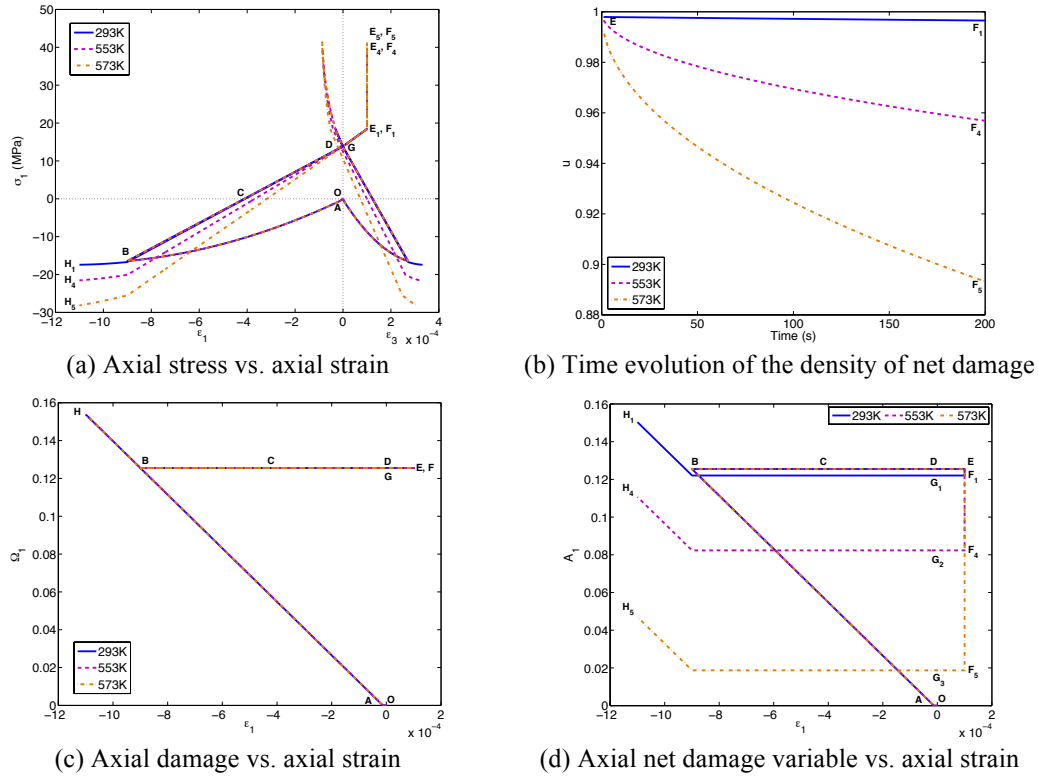


**FIG. 4 Stress path simulated for a 200s healing period under three temperatures.**

#### 4. CONCLUSION

A theoretical framework is proposed to model crack opening, closure and healing in rock under thermo-mechanical (TM) stresses. The model is based on Continuum Damage Mechanics (CDM), with damage defined as the second-order crack density tensor. The free energy is postulated as a polynomial of deformation, temperature, damage and healing. The proposed damage-driving force captures damage evolution as well as the decrease of material toughness at elevated temperature. Crack closure is modeled by adopting the concept of unilateral effect. A mixed variable is introduced to account for anisotropic TM damage and rate-dependent healing. The healing evolution law is governed by diffusion equation and requires the introduction of an internal length parameter relating to the average crack spacing in the Representative

Elementary Volume (REV). Healing depends both on time and temperature. The healing deformation describes the difference between REV deformation before and after the DMT process. A numerical study is performed to compute the degradation and recovery of strength and stiffness in the damaged medium. Unilateral effects result in stiffness recovery during compressive stress paths. The model also captures stiffness recovery and compensation of damage-induced irreversible deformation. A parametric study illustrates the model capabilities, mainly: the simulation of TM stress paths with higher degree of mechanical recovery for longer healing time or higher healing temperature. The proposed model is expected to better predict the long-term behavior of self-healing rock materials. Further studies will be dedicated to the proper calibration and validation of the model for salt rock.

## REFERENCES

- Arson, C., Xu, H., and Chester, F.M. (2012). "On the definition of damage in time-dependent healing models for salt rock." *Géotechnique Letters*. 2 (2): 67-71.
- Barbero, E.J., Greco, F., and Lonetti, P. (2005). "Continuum damage-healing mechanics with application to self-healing composites." *Int. J. Damage Mech.* 14 (1): 51-81.
- Chaboche, J.L. (1992). "Damage induced anisotropy: on the difficulties associated with the active/passive unilateral condition." *Int. J. Damage Mech.* 1 (2): 148-171.
- Chan, K.S., Bodner, S.R., and Munson, D.E. (1998). "Recovery and healing of damage in WIPP salt." *Int. J. Damage Mech.* 7 (2): 143-166.
- Dragon A, Halm D, and Désoyer T. (2000). "Anisotropic damage in quasi-brittle solids: modeling, computational issues and applications." *Comput Methods Appl Mech Eng.* 183 (3): 331-352.
- Hou, Z. (2003). "Mechanical and hydraulic behavior of rock salt in the excavation disturbed zone around underground facilities." *Int. J. Rock Mech. Min. Sci.* 40 (5): 725-738.
- Kachanov, M. (1992). "Effective elastic properties of cracked solids: critical review of some basic concepts." *Appl. Mech. Rev.* 45 (8): 304-335.
- Miao, S., Wang, M., and Schreyer, H. (1995). "Constitutive models for healing of materials with application to compaction of crushed salt." *J. Eng. Mech. (ASCE)*. 121 (10): 1122-1129.
- Senseny, P.E., Hansen, F.D., Russell, J.E., Carter, N.L., and Handin, J.W. (1992). "Mechanical behavior of rock salt: phenomenology and micromechanisms." *Int. J. Rock Mech. Min. Sci. Geomech. Abstr.* 29 (4): 363-378.
- Voyiadjis, G.Z., Shojaei, A., Li, G., and Kattan, P.I. (2012). "A theory of anisotropic healing and damage mechanics of materials." *Proc. R. Soc. A.* 468 (2137): 163-183.
- Yu, W. and Fuji, A. (2000). "Diffusion of  $Tl^+$  ions through the interface of solid NaCl or KCl and liquid  $TlCl$ ." *Proc. 7<sup>th</sup> Asian. Conf. Solid. State. Ionics*. Fuzhou: 129-133.
- Zhu, C. and Arson, C. (2013). "Modeling the influence of thermo-mechanical crack opening and closure on rock stiffness." *Proc. 5<sup>th</sup> Biot Conf. Poromech.* Vienna, Austria, 10-12 July, 2013, p.2526-2535.